ARTICLES

Stacking-fault energy of copper from molecular-dynamics simulations

P. Heino*
Tampere University of Technology, Institute of Electronics, P.O. Box 692, FIN-33101 Tampere, Finland

L. Perondi† and K. Kaski
Helsinki University of Technology, Laboratory of Computational Engineering, P.O. Box 9400, 02015 HUT, Finland

E. Ristolainen
Tampere University of Technology, Institute of Electronics, P.O. Box 692, FIN-33101 Tampere, Finland

(Received 2 July 1999)

The behavior of the energy of stacking fault defects in copper as a function of external strain and temperature is investigated making use of molecular-dynamics simulations. Atomic interactions are modeled by an effective-medium theory potential. Intrinsic, extrinsic, and twinning faults are considered. Our results suggest that the stability of stacking-fault defects in copper increases with temperature and decreases with applied compressive strain. In addition, we point out some difficulties posed by the application of finite range model potentials to the study of low-energy defects. To show that these difficulties are quite general in nature we also compute the stacking-fault energy (SFE) from an embedded atom model potential. Our results indicate that the SFE computed from model potentials displays a spurious change of sign with increasing compressive strain. [S0163-1829(99)02245-6]

I. INTRODUCTION

In the theory of deformation[1] of fcc crystals, stacking-fault defects play an important role in processes such as work hardening.[2,3] The stacking-fault energy (SFE) is directly related, for example, to the dissociation of dislocations into two Shockley partials and to the energetics of crystal twinning. Accordingly, great effort has been directed to the study of stacking-fault defects, both experimentally and theoretically (see Ref. 4, and references in Table I). Experimentally, the SFE is usually measured from the mutual distance of partial dislocations,[5] and its temperature dependence can be determined for instance from x-ray measurements.[6] However, we are not aware of studies to measure or calculate the dependence of the SFE on the state of strain of the sample. Such studies would provide further insight into the dynamics of dislocations.

The mobility of dissociated dislocations in a stressed sample, mainly the ability of screw dislocations to cross-slip, is critically dependent on the distance between the partials. This distance, in turn, is determined by the SFE, which may vary with the local state of stress. Results from recent simulations, aimed at the study of dislocation emission in small copper systems,[7] suggest that there may, in fact, be a noticeable dependence of the stacking-fault energy on the local state of stress. One of the purposes of this paper is to investigate the extent of this dependence, for small values of strain, and how it is affected by temperature. To this effect, we study the dependence of the stacking-fault energy of copper on strain and temperature making use of the molecular-dynamics simulation method.[8]

Our second objective is to call the attention for the subtle fact that even otherwise realistic model potentials may give rise to the wrong sign for the SFE when applied to materials under a small compressive strain. More explicitly, we show that the SFE computed from two model potentials, namely, the embedded atom model (EAM) and the effective-medium theory (EMT) potential, displays a spurious change of sign with increasing compressive strain. We will argue that this failure is a consequence of the finite range of the potential. Although our results are restricted to metals, we believe that the conclusions drawn from them are quite general in nature.

The paper is organized as follows. Basic aspects of the EMT and EAM model potentials are described in Sec. II. Section III is dedicated to the description of the procedure followed in the simulations as well of the studied defects. In Sec. IV we show and discuss our results for the SFE as a function of both temperature and strain. In Sec. V, we show that the SFE may change sign with increasing strain and argue that this is an artifact of the finite range of the model potential. Finally, in Sec. VI we draw conclusions.

II. POTENTIAL MODEL

The many-atom nature of metallic cohesion is crucial in describing the mechanical properties of metals. Accordingly, many-atom potentials show clear advantages over classical pair potentials. EMT and EAM model potentials are examples of many-atom potentials, which have been extensively used in the study of metals.[9,10]

Details about the EMT potential used in this paper may be found in Ref. 11. In the EMT, the total energy of a system

consisting of N metal atoms is expressed as

$$E=\sum_{i}^{N} E_C(\overline{n_i})+E_{AS}, \tag{1}$$

where the first term is the sum of individual ''embedding energies'' $E_C(\overline{n_i})$, and $\overline{n_i}$ is the averaged background electron density over a sphere centered at atomic site i. For finite temperatures and for systems with a more open lattice structure, the atomic-sphere correction term E_{AS} accounts for the overlaps and neglected interstitial volume of the atomic spheres. Compared to other many-atom potentials for metals, EMT has a strong *ab initio* nature since, in principle, the parameters in the total-energy expression can be calculated using the jellium model. In practice, however, one experimental parameter, namely, the value of the elastic constant c_{44}, is used in the actual calculations.[12] As previously, we use a modification of the original EMT scheme, which extends the atomic interactions up to the third neighbors in an fcc lattice.[11]

The total energy in the EAM scheme is expressed as

$$E=\sum_{i}^{N} G_i\left(\sum_{j\neq i}\rho_j(R_{ij})\right)+\frac{1}{2}\sum_{i\neq j}U(R_{ij}), \tag{2}$$

where G is the embedding energy, its argument, $\Sigma_{j\neq i}\rho_j(R_{ij})$, is the electron density at site i, and U is a two-atom electrostatic interaction. The embedding energy, together with the electron density at a given site are obtained as follows. Educated guesses for the parameters of functions ρ and U are defined. Then, with the aid of an empirical function for E (Ref. 13) and by fitting quantities derived from Eq. (2) to known experimental values of properties of the metal in question, the parameters defining ρ and U are obtained. Finally, by varying the lattice parameter, a numerical relation between G and ρ is obtained for a range of values of ρ. For more details about this procedure, we refer the reader to Refs. 10, 14, and 15. It should be emphasized that there are similarities between EMT and EAM model potentials, as discussed in Ref. 11.

III. DEFINITION OF THE SIMULATION MODEL

In a defect-free fcc structure, three types of close-packed {111} planes that are displaced relative to one another and denoted by A, B, and C, are stacked in the following sequence $ABCABC\ldots$. One example of a stacking fault is formed when, from a given plane on, the A planes are moved to the position of B planes, the B planes to the position of C planes, and so on. In the fcc lattice, this is equivalent to displacing all layers from a given point on by $a/6[11\overline{2}]$, where a is the lattice parameter. Hence, the $ABCABCAB\ldots$ structure changes to $ABCBCABC\ldots$, when the fourth layer suffers a slip. The fault thus formed is termed an intrinsic stacking fault (SF). If, now, the subsequent layer is subjected to a slip an extrinsic SF, $ABCBABCA\ldots$, is formed. If we continue, in this way, slipping subsequent layers then eventually a twin is generated, where half the crystal has the stacking sequence ABC and the other half CBA. It should be reminded that the hexagonal close-packed structure (hcp) is closely related to the fcc structure. The hcp symmetry is generated by stacking the {111} planes in the $ABABAB\ldots$ stacking sequence. Thus, when an fcc lattice contains stacking faults, it may be said that some of its layers are in the environment of an hcp structure. Therefore, the SFE is closely related to the stability of the fcc crystal structure.

In our computations of the SFE as a function of temperature and strain, the temperature was set through a Nosé-Hoover thermostat.[16] Different states of strain were included through dilation of the lattice, as described in detail below. The energy of the fault has been computed from the following equation:[17]

$$\gamma=\frac{E'-NE_0}{A}, \tag{3}$$

where E' is the total potential energy of the system containing the SF, N is the number of atoms in the system, E_0 is the energy per atom in a defect free system and A is the area of the faulty plane.

At temperatures greater than 0 K, the energies in the above equation include the kinetic energy, and have been computed as a time average such that the higher the temperature, the longer the total time for averaging. For the highest temperature studied, $T=700$ K, averages were performed over a time span of about 40 ps.

The calculations were performed in a structure generated by applying periodic boundary conditions, in all directions, to a simulation box with faces (111), $(1\overline{2}\overline{2})$, and $(01\overline{1})$. The dimensions of the simulation box were chosen such that the atoms about half the distance away separating two periodic images of the stacking fault plane could be considered as atoms in the bulk. This was checked by direct computation of the potential energy of those atoms.

In the perfect fcc lattice, periodic boundaries in the $[111]$ direction are implemented by choosing the number of {111} planes equal to $3M$. For a system with an intrinsic fault, $3M-1$ such planes must be used while for a system with an extrinsic fault, $3M-2$ planes are necessary. In our studies the system size is equal to 36, 35, 37, 36, and 38 for a structure containing 0, 1, 2, 3, and 4 slips, respectively. The energy of a twin structure was computed from a system containing 42 {111} planes. In all simulations, the dimensions of the system in the other two orientations, i.e., $[2\overline{11}]$ and $[01\overline{1}]$, were 43 and 39 Å, respectively. In our simulations the total number of atoms was always around 13 000 atoms, and the zero-pressure lattice constant, for different temperatures, was taken from Ref. 11.

Two types of strain states were studied: extension or compression in the $[111]$ direction only (when the size in other directions is kept fixed) and uniform extension or compression, when the strain is uniform in all directions. Strain was imposed by rescaling the zero-pressure coordinates (and the periodic size) with a factor $1+\epsilon$, where ϵ is the value of the strain. Computations were performed for eleven different values of the strain in the interval of -3% to 3%.

IV. RESULTS AND DISCUSSION

A. Energy profile of the planes near a fault

It is noticed that if only geometrical aspects of the system were taken into account, i.e., making a nearest-neighbor ap-

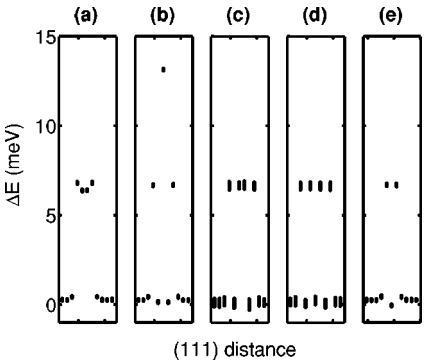

FIG. 1. The energy of atoms (meV above $E_0 = -3.56$ eV) as a function of their location in the [111] direction. The system contains an intrinsic (a), extrinsic (b), 3-slip (c), 4-slip (d), or a twin (e) fault of the type shown in Fig. 2. Results for copper, computed from the EMT model potential.

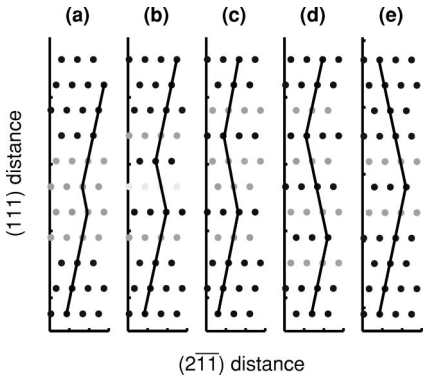

FIG. 2. The energy of atoms as a function of their location in the vertical [111] and horizontal [$2\bar{1}\bar{1}$] directions. Shading indicates the energy, cf. Fig. 1. The lines serve as guides to the eye indicating 1-, 2-, 3-, and 4-slip faults and a twin fault in subfigures (a)–(e), respectively. The lines show the *ABC* and *CBA* stacking sequences, at the boundary of a layer of atoms is in the hcp structure, indicated by an edge of the line. Results for copper, computed from the EMT model potential.

proximation, the energy of an intrinsic fault (γ) would be equal to that of an extrinsic fault and both would have twice the energy of a twin boundary.[18,19] Although the quantitative results obtained with the EMT model agree quite well with this approximation, the effect of layers beyond the nearest one shows up in several circumstances. For instance, Figs. 1 and 2 show the energies of the atoms as a function of their location with respect to the faulty plane. It is evident that the SFE may not be obtained simply by counting the number of (111) layers in the hcp structure (i.e., *B* layers in the *ABA* structure). Especially, in the structure containing an extrinsic fault, the atomic energy is highest at the plane in the middle of the fault, in an fcc lattice environment. In addition, the energies of 3-slip and 4-slip faults [subfigures (c) and (d)] are equal, but both are about 18% less than γ, which represents a significant deviation from a nearest-neighbor model. Also, in the case of the twin fault, the SFE comes from *two* atomic layers, those that surround the one in the hcp structure environment.

Hence, although a nearest-neighbor model may result in quite good quantitative agreement for the energy of faults, it does not at all give a good description of the atomic configuration near the faults. This is a relevant factor when studying the effect of faults on diffusion or on other properties that strongly depend on the local configuration of atoms. Next we will discuss the effect of temperature and strain on the faults' energy.

B. Temperature dependence

In Table I, we present our results for the intrinsic stacking-fault energy of copper for temperatures $T = 1$ K and $T = 300$ K. Several other theoretical and experimental values for this quantity are also quoted in this same table. Most theoretical values are based on minimum-energy calcula-

TABLE I. Stacking-fault energy of copper in units of (ergs/cm^2) taken from different references. The letters (*t*) and (*e*) indicate whether the value is theoretical or experimental, respectively. (*) in the reference indicates *not* the original reference, but a collection, the publication year of which is in brackets.

	Type	Intrinsic	Extrinsic	Twin
This work, $T = 1$ K	(*t*)	78.1	78.5	39.3
This work, $T = 300$ K	(*t*)	64.6		
(1993) (Ref. 19)	(*t*)	56	57	26
(1990) (Ref. 23)	(*t*)	70	73	36
(1992) (Ref. 25)	(*t*)	50	44	29
(1966) (Ref. 5)	(*t*)	30		
(1972) (Ref. 22), $T = 973$, 1073, 1148, 1173 K	(*e*)			25,24,22,21
(1970) (Ref. 26), $T = 973$	(*e*)	70		26
(1971) (Ref. 27), $T = 1148$ K	(*e*)			21
(1965) (Ref. 28), $T = 293$ K	(*e*)	50 ± 6		
(1951)* (Ref. 20), $T = 1218$ K	(*e*)	40		
(-1970)* (Ref. 20)	(*e*)	30, . . . ,160,55		
(1971) (Ref. 21), $T =$ room(?)	(*e*)	41		
(1961) (Ref. 29), $T =$ room(?)	(*e*)	40		
(1965) (Ref. 30), $T = 988$ K	(*e*)	71.9		44.1
(1961) (Ref. 31), $T = 1223$	(*e*)			12

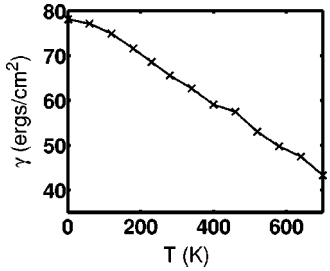

FIG. 3. Stacking-fault energy, γ, for copper as a function of temperature, at zero strain. Result computed from the EMT model potential with an abrupt cutoff radius.

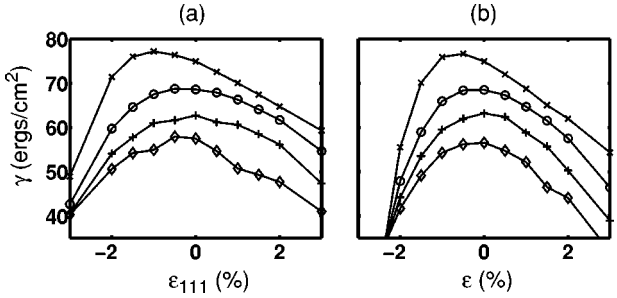

FIG. 4. Stacking-fault energy for copper, γ, as a function of external strain. (a) Anisotropic strain perpendicular to the (111) plane. (b) Isotropic strain in all directions. Four temperatures are shown: $T=120$ K ($\times$), $T=230$ K ($\bigcirc$), $T=340$ K ($+$), and $T=460$ K ($\diamond$). Results computed from the EMT model potential.

tions, and as such correspond to zero temperature. With respect to the experimental values it happens quite often that the temperature at which the measurements are carried out is *not* given in the references, which is somewhat disappointing regarding our objectives. Fortunately, however, in some cases the value of the temperature may be inferred from the type of experiment used to measure the energy of the fault. When the SFE is measured from the ratio of the twin boundary energy and the average grain-boundary energy, high temperatures (about 1000 K) are necessary (cf., e.g., Ref. 20). Another method is based on determining the distance between the dissociated partial dislocations from micrographs, such as in Ref. 21. In these measurements the temperature is most probably near the room temperature. Because the SFE decreases with increasing temperature,[6,22] a direct comparison of a minimum-energy SFE and the experimental SFE might be somewhat misleading. It seems that the relation $\gamma = 2\gamma_{twin}$ holds with reasonable accuracy in all circumstances, though Gallagher[20] pointed out that this may slightly underestimate the true SFE.

From our results, it is seen that they show reasonable agreement with some of the experimental data. The zero-temperature result for the intrinsic stacking fault tends to be somewhat larger than the other theoretical values, although there is a quite large dispersion among them. Note that the value given in Ref. 23 is quite close to the result obtained in the present calculation. From the experimental values in the table it is seen that the measured value of the SFE decreases with increasing temperature. The rate of change of the SFE with temperature, $d\gamma/dT$, was reported to be -0.02 ergs/(cm^2 K) by Murr.[22] Shetty[6] gave this value proportional to the SFE at 300 K. Using the SFE value at 300 K proposed by Murr, the temperature coefficient obtained from Shetty's estimative is -0.06 ergs/(cm^2 K). The value we obtain for temperatures above 120 K is -0.05 ergs/(cm^2 K), which is in very good agreement with the empirical coefficients given by Murr and Shetty. The results of our simulations for the behavior of the SFE with temperature, in the range 0–700 K, are given in Fig. 3. It is seen that the EMT approximation predicts a breakdown of the linear dependency at low temperatures (120 K).

To summarize, the results given by the EMT for both the SFE and its temperature dependence are in quite good agreement with experimental data. This indicates that in copper the stability of stacking faults increases with temperature. It is important to note that the temperature behavior of the SFE in a given material may change quite substantially when impurities are added to the material. For instance, experimental results given in Ref. 24 show that Cu doped with a low concentration of Al gives an SFE that increases with temperature. However, if the concentration of Al is further increased, the SFE increases up to temperatures around 700 K and, then, begins to decrease.

C. Strain dependence

The study of the dependence of the SFE on the state of strain is one of the main purposes of this work. In an earlier simulation,[7] where a cylindrical copper system was sheared, we obtained some indications that the SFE would change noticeably with the state of strain. Since the SFE plays an important role in the motion of dislocations, mainly in their ability to cross-slip, it seemed to us that studying how the SFE changes with the state of strain would give further insight into the dynamics of dislocations and, consequently, in the mechanisms of plastic deformation in a strained sample. Despite this apparent importance of the effect of the state of strain on the SFE, we are not aware of studies to measure or to give a quantitative estimate for it. These facts have specially motivated the present study.

In our studies, we have investigated two situations: strain is isotropically imposed in all three perpendicular directions (isotropic) and strain is applied in the [111] direction only (anisotropic). The strain states described above are imposed by rescaling the atomic positions with a factor $(1+\epsilon)$. Results for eleven different values of ϵ were computed: $\epsilon \in \{\pm 3\%, \pm 2\%, \pm 1.5\%, \pm 1\%, \pm 0.5\%, 0\%\}$.

The results, for different values of temperature, are shown in Fig. 4(a) for the case of anisotropic strain and in Fig. 4(b) for the case of isotropic strain. From the figures it is seen that, independently of temperature, the SFE monotonically increases with compressive strain up to a maximum and then suddenly begins to decrease towards negative values. In the next section, we will argue that this maximum and subsequent decreasing of the SFE are an artifact of the finite range of the potential. According to our interpretation, therefore, the SFE increases with increasing compressive strain and Figs. 4(a) and 4(b) show a qualitatively correct picture only for values of strain smaller than the strain corresponding to the maximum of the SFE. From the results, it is also seen that temperature has the effect of decreasing the SFE for all values of strain. If these results were correct, one would expect dislocations to move more easily when under compres-

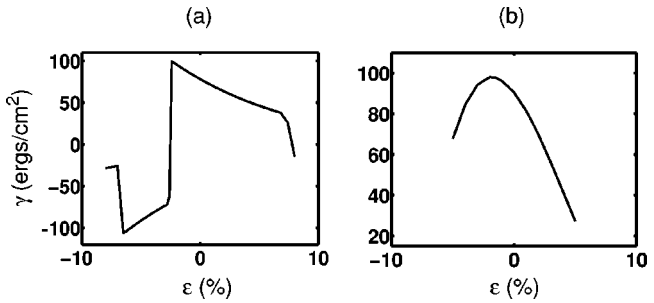

FIG. 5. Zero-temperature stacking-fault energy, γ, as a function of isotropic strain (a) for copper, computed from the EMT potential, and (b) for aluminum, computed from the EAM potential.

sive strain, provided that the positive effect of closer partials on mobility is not overcome by the negative effect caused by an increased Peierls barrier.[32]

Another observation is that the dependence of the SFE on temperature is much stronger than one might expect from thermal expansion. For example, a temperature increase from 120 to 700 K changes the zero-pressure lattice constant from 6.609 to 6.682 (Ref. 11) and may be thought as equivalent to a uniform tension of 1.11% for the system at 120 K. This increase in the temperature decreases the SFE from 75 to 43 ergs/cm^2 (cf. Fig. 3), which is substantially smaller than the value of the SFE in a system at 120 K with 1.11% uniform elongation [about 70, as seen in Fig. 4(b)].

D. Failure of model potentials in describing the SFE

Model potentials, derived either by using an EMT or EAM approach, have a cutoff radius beyond which the potential is set to zero. The introduction of such a finite range in the potential greatly improves the performance of molecular-dynamics simulations. This gain in performance, however, causes a loss in the accuracy with which energies are computed. It is our objective in this section to give evidence that this loss in accuracy may have, in some circumstances, quite catastrophic consequences when computing structural energies in samples subjected to compressive strain. As advanced in the Introduction, we will illustrate this point by considering examples given by SF defects.

Figures 5(a) and 5(b) show the zero-temperature energy of an intrinsic SF defect as a function of isotropic strain computed from the EMT and EAM model potentials, respectively. Note that the EAM result is obtained for aluminum rather than copper: the energy obtained from the EAM potential, in the implementation given in Ref. 15, for intrinsic stacking-fault defects in copper is negative, indicating that this potential favors an hcp structure for copper.

The EMT result, in Fig. 5(a), shows that the SFE increases with increasing compressive strain up to a *critical strain*, where it abruptly drops to negative values. If true, this transition would indicate that the material undergoes a structural transition at this point, changing from the fcc lattice structure to the hcp structure—all dislocations in fcc structure would completely dissociate. It is known,[33,34] however, that none of the simple metals with fcc lattice undergoes a phase transition for linear deformations smaller than at least 12%. Hence, the abrupt drops in SFE, see Fig. 5(a), are an artifact of the potential. This result has been computed with a version of the EMT potential in which an abrupt cutoff radius has been used. Also a continuous cutoff for the EMT potential has been proposed in Ref. 35. However, that implementation gives negative values for the SFE of copper. The sudden changes in the SFE, as will be clear in the forthcoming discussion, are due to the discontinuous variation of the potential at the cutoff radius.

TABLE II. Coordination shells of the fcc lattice and the hcp structure. The letters N and d stand for the number of atoms and the radius in lattice units, respectively, of the shell whose order is specified in the first column. The cutoff radius of the EMT potential, 1.319 in units of the lattice parameter, is located between the third and fourth coordination shells of the fcc lattice. The corresponding value for the EAM potential, 1.663, is located between the fifth and sixth coordination shells of the fcc lattice.

Coordination shell	fcc lattice		hcp structure	
	N	d	N	d
1	12	0.707	12	0.707
2	6	1.000	6	1.000
			2	1.155
3	24	1.225	18	1.225
			12	1.354
4	12	1.414	6	1.414
5	24	1.581	12	1.581
			12	1.683
6	8	1.732	6	1.732
			6	1.779
			12	1.825
7	48	1.871	24	1.871
			6	1.915
8	6	2.000		
			12	2.041
9	36	2.121	12	2.121
			24	2.195
10	24	2.236	12	2.236
			12	2.273
			2	2.309

Figure 5(b) shows the result for an EAM potential. Here, as with the EMT potential, the SFE becomes negative for compressive strain beyond a given limit. This shows that model potentials, derived either by using an EAM or EMT approach, show similar problems in the SFE for increasing values of compressive strain. The maximum of SFE and the smooth transition from positive to negative values, seen in the EAM result, is a consequence of the fact that in this case a smooth cutoff has been implemented. An explanation for these changes in the sign of the SFE, independent of the model potential, may be given in terms of the finite range of the potential and differences in the coordination numbers between the fcc and the hcp lattice structures.

Table II gives the number of atoms in each coordination shell of both the fcc and the hcp structures. The coordination shells of the fcc structure have been numbered in the first column. The positions of the cutoff radius of the EMT and EAM model potentials are indicated in the caption of the figure. In what follows, we will refer to the atoms that interact with a particular atom as interacting atoms. With increas-

ing compressive strain, the lattice shrinks and the number of interacting atoms abruptly increases each time the radius of the next outer coordination shell gets smaller than the cutoff radius. For instance, at zero strain, the cutoff radius of the EMT potential is localized between the third and fourth coordination shells of the fcc lattice and below the coordination shell of the hcp structure with radius 1.354 (see Table II). In this situation, the total number of interacting atoms in the fcc structure is 42 while that in the hcp structure is 38. When compressive strain is applied, at some point the fifth coordination shell in the hcp structure becomes smaller than the cutoff radius. At this point, the number of interacting atoms in the hcp structure jumps from 38 to 50, outnumbering those in the fcc lattice. As a result of the fact that the cohesion energy in all model potentials increases with the number of interacting atoms, at this level of strain the hcp structure becomes more stable than the fcc lattice and thus the SFE shows a change of sign. Another way of characterizing this effect is to say that the SFE, computed from a model potential in an fcc lattice, depends on the cutoff radius. The value of the *critical compressive strain*, where the abrupt change in energy takes place, is defined by the relative position of the cutoff radius with respect to the coordination shells of both the fcc lattice and hcp structure.

The failure of the model potential in giving the correct sign for the SFE is *not* restricted to compressive strains. From Fig. 5(a) it is seen that the SFE decreases rapidly and changes sign at high tensile strains. This is the result of the third coordination shell moving outside the cutoff sphere of the potential. As a result, for such a large tensile strain, the hcp structure contains 20 interacting atoms compared to 18 in the fcc. Due to cohesion, as discussed above, the SFE becomes negative. However, because of the exponential decay of the potential and the small number (two) of interacting atoms in favor for the hcp structure, the absolute value of the SFE becomes relatively small, about -2 ergs/cm^2. Following the above reasoning, the strain values ϵ_c, at which these transitions should happen are found from $1.354(1+\epsilon_c)=r_c$ and $1.225(1+\epsilon_c)=r_c$, where the cutoff radius is in the middle between the third and fourth neighbors of the fcc lattice, i.e., $r_c=1.132$. Thus, the strain values ϵ_c for these transitions should be -2.5% or 7.7%. As seen from Fig. 5(a), these transitions occur exactly there.

Although not with the details given here, the above points have already been remarked by other authors.[36,37] Most of the events associated to deformation of materials may be related to dislocations and their dynamics. The above results show that model potentials may give a wrong description of the structure of dislocations and their motion, in the whole material sample or in a particular region of it, when the compressive strain exceeds the critical strain for changes in the number of interacting atoms, as discussed above. Thus, care must be exercised when interpreting the results of simulations that involve model potentials.

V. SUMMARY

We have studied the temperature and strain dependence of the stacking-fault energy of copper, by using the molecular-dynamics method and a model potential based on the effective-medium theory. The results obtained with this model potential, with the given cutoff radius, are in quite good agreement with experimental results. The stacking-fault energy was seen to decrease with increasing temperature and to increase under compressive strain. Taking the SFE as a measure of the separation between partials, these results indicate that the mobility of dislocations decreases with temperature and increases with compressive strain, as far as the separation into partials is concerned. The above facts indicate that the EMT model potential, in the implementation given in this paper, is suitable for the study of dislocation motion in fcc metals, but limited to the low compressive and moderate tensile strain regime.

As a second result of our studies, we have shown that model potentials fail to give the correct sign of the SFE in fcc lattices, when the material is subjected to either compressive or tensile strain, beyond given limits. This failure may be traced to the finite range imposed on these potentials. The level of compressive strain at which the SFE changes sign depends on the value of the cutoff radius of the model potential and on the lattice parameter. If the model potential gives a discontinuous energy at the cutoff radius, the change in the SFE will be abrupt. Otherwise, if the energy change is continuous at the cutoff radius, the SFE shows a behavior that resembles a parabola with negative curvature. In this case, the transition from positive to negative values of the SFE is continuous for all values of compressive strain.

*Author to whom correspondence should be addressed. Electronic address: Pekka.Heino@ele.tut.fi

†Permanent address: Instituto Nacional de Pesquisas Espaciais–INPE, P.O. Box 515, 12-227-010 São José dos Campos–SP, Brazil.

[1] J. P. Hirth and J. Lothe, *Theory of Dislocations* (McGraw-Hill, New York, 1968).

[2] D. Kuhlmann-Wilsddorf, Philos. Mag. A **79**, 955 (1999).

[3] R. Hertzberg, *Deformation and Fracture Mechanics of Engineering Materials* (Wiley, New York, 1989).

[4] V. Paidar, in *Proceedings of the Symposium on the Structure and Properties of Crystal Defects*, edited by V. Paidar and L. Lejček (Elsevier, Amsterdam, 1983).

[5] R. M. Cotterill and M. Doyama, Phys. Rev. **145**, 465 (1966).

[6] M. N. Shetty, Z. Metallkd. **72**, 648 (1981).

[7] P. Heino and E. Ristolainen, Nanostruct. Mater. **11**, 587 (1999).

[8] M. P. Allen and D. J. Tildesley, *Computer Simulation of Liquids* (Oxford University Press, Oxford, 1987).

[9] K. W. Jacobsen, J. K. Nørskov, and M. J. Puska, Phys. Rev. B **35**, 7423 (1987).

[10] M. S. Daw, S. M. Foiles, and M. Baskes, Mater. Sci. Rep. **9**, 251 (1993).

[11] H. Häkkinen and M. Manninen, J. Phys.: Condens. Matter **1**, 9765 (1989).

[12] K. W. Jacobsen, Comments Condens. Matter Phys. **14**, 129 (1988).

[13] J. H. Rose, J. R. Smith, F. Guinea, and J. Ferrante, Phys. Rev. B **29**, 2963 (1984).

[14] S. Chantasiriwan and F. Milstein, Phys. Rev. B **53**, 14 080 (1996).

[15] S. Chantasiriwan and F. Milstein, Phys. Rev. B **58**, 5996 (1998).

[16] S. Nosé, Suppl. Prog. Theor. Phys. **103**, 1 (1991).

[17] H. Häkkinen, S. Mäkinen, and M. Manninen, Phys. Rev. B **41**,

12 441 (1990).
[18] W. T. Read, *Dislocations in Crystals* (McGraw-Hill, New York, 1953).
[19] N. M. Rosengaard and H. L. Skriver, Phys. Rev. B **47**, 12 865 (1993).
[20] P. C. J. Gallegher, Metall. Trans. A **1**, 2429 (1970).
[21] W. M. Stobbs and C. H. Sworn, Philos. Mag. **24**, 1365 (1971).
[22] L. E. Murr, Scr. Metall. **6**, 203 (1972).
[23] S. Crampin, K. Hampel, and D. D. Vvedensky, J. Mater. Res. **5**, 2107 (1990).
[24] T. Imura and H. Saka, in *Proceedings of the Symposium on the Structure and Properties of Crystal Defects* (Ref. 4).
[25] G. Schweizer, C. Elsässer, K. Hummler, and M. Fähnle, Phys. Rev. B **46**, 14 270 (1992).
[26] L. E. Murr, Phys. Status Solidi A **3**, 447 (1970).
[27] R. A. Queeney, Scr. Metall. **5**, 1031 (1971).
[28] Von E. Peissker, Acta Metall. **13**, 419 (1965).
[29] A. Howie and P. R. Swann, Philos. Mag. **6**, 1215 (1961).
[30] C. G. Valenzuela, Trans. Metall. Soc. AIME **233**, 1911 (1965).
[31] M. C. Inman and A. R. Khan, Philos. Mag. **6**, 937 (1961).
[32] W. A. Jesser and D. Kuhlmann-Wilsddorf, Mater. Sci. Eng. **9**, 111 (1972).
[33] J. Xu, H. Mao, and P. M. Bell, High Temp.-High Press. **16**, 495 (1984).
[34] U. Walzer, High Temp.-High Press. **19**, 161 (1987).
[35] H. Häkkinen and M. Manninen, Phys. Rev. B **46**, 1725 (1992).
[36] K. Stokbro and K. W. Jacobsen, Phys. Rev. B **47**, 4916 (1993).
[37] H. Häkkinen and M. Manninen, Phys. Scr. **T33**, 210 (1990).